

# INVESTIGATION OF DALTON AND AMAGAT'S LAWS FOR GAS MIXTURES WITH SHOCK PROPAGATION

PATRICK WAYNE<sup>1</sup>, SEAN COOPER<sup>1</sup>, DYLAN SIMONS<sup>1</sup>, IGNACIO TRUEBA MONJE<sup>2</sup>, JAE HWUN YOO<sup>3</sup>, PETER VOROBIEFF<sup>1</sup>, C. RANDALL TRUMAN<sup>1</sup> & SANJAY KUMAR<sup>4</sup>

<sup>1</sup>Department of Mechanical Engineering The University of New Mexico, Albuquerque, New Mexico, USA.

<sup>2</sup>Department of Mechanical and Aerospace Engineering Ohio State University Columbus, Ohio, USA.

<sup>3</sup>Department of Aerospace Engineering University of Illinois Urbana, Illinois, USA.

<sup>4</sup>Department of Aerospace Engineering Indian Institute of Technology Kanpur Kanpur, Uttar Pradesh, India.

## ABSTRACT

Dalton's and Amagat's laws (also known as the law of partial pressures and the law of partial volumes respectively) are two well-known thermodynamic models describing gas mixtures. Our current research is focused on determining the suitability of these models in predicting effects of shock propagation through gas mixtures. Experiments are conducted at the Shock Tube Facility at the University of New Mexico (UNM). The gas mixture used in these experiments consists of approximately 50% sulfur hexafluoride (SF<sub>6</sub>) and 50% helium (He) by moles. Fast response pressure transducers are used to obtain pressure readings both before and after the shock wave; these data are then used to determine the velocity of the shock wave. Temperature readings are obtained using an ultra-fast mercury cadmium telluride (MCT) infrared (IR) detector, with a response time on the order of nanoseconds. Coupled with a stabilized broadband infrared light source (operating at 1500 K), the detector provides pre- and post-shock line-of-sight readings of average temperature within the shock tube, which are used to determine the speed of sound in the gas mixture. Paired with the velocity of the shock wave, this information allows us to determine the Mach number. These experimental results are compared with theoretical predictions of Dalton's and Amagat's laws to determine which one is more suitable.

*Keywords: Amagat's law, compressibility, Dalton's law, gas mixture, shock waves.*

## 1 INTRODUCTION

Dalton's law was observed in 1801 by an English chemist, physicist and meteorologist John Dalton. In 1802, he reported his findings [1] in *Memoirs of the Literary and Philosophical Society of Manchester*. This law of additive (partial) pressures states that the total pressure of a gas mixture is equal to the sum of the pressures each gas would exert if it existed alone at the mixture temperature and pressure.

In 1880, a French physicist Emile Hilaire Amagat published his findings while researching the compressibility of different gases. Amagat's law of additive (partial) volumes is similar to Dalton's law, stating that the total volume of a gas mixture is equal to the sum of the volumes each gas would occupy if it existed alone at the temperature and pressure of the mixture [2]. Although science has evolved considerably since the 1800s, very little is known about the behavior of multicomponent gases in various conditions, especially when these gases experience near-instantaneous increases (or decreases) in properties such as pressure, density, and temperature.

The goal of the experiment described here is to determine the accuracy of Dalton's law and Amagat's law in prediction of the properties of a gas mixture subject to shock wave propagation. Shock wave effects on gaseous mixtures are important not only for the fundamental understanding of the physics involved, but also for real-world applications such as scramjet/ramjet engine inlets [3], and pneumatic systems and piping [4]. These experimental data can also be used for numerical validation to better predict these effects in computational fluid dynamics (CFD) simulations.

## 2 THEORY

Dalton's law and Amagat's law can be expressed by the following equations:

$$\text{Dalton's law:} \quad P_m = \sum_{i=1}^k P_i(T_m, V_m) \quad (1)$$

$$\text{Amagat's law:} \quad V_m = \sum_{i=1}^k V_i(T_m, P_m) \quad (2)$$

where  $P_i$  and  $V_i$  correspond to pressure and volume of the individual gas components,  $P_m$  and  $V_m$  correspond to the pressure and volume of the gas mixture, and  $T_m$  is the temperature of the mixture. A system obeying eqn. (1) exactly is known as an ideal mixture, irrespective of whether its components individually behave as ideal gases [5]. The ideal gas equation of state (EOS) is expressed as  $PV = nRT$ , where  $n$  = the amount of the gas (in moles) and  $R = 8.314$  J/mol K is the universal gas constant. For ideal gas systems, both eqns. (1) and (2) provide exact results, but only approximate solutions for real gases, due to intermolecular forces, compressibility, and non-equilibrium thermodynamic effects. Real gases can be expressed more precisely by a modified form of the ideal gas EOS,

$$PV = znRT \quad (3)$$

$$z = \frac{PV}{nRT} \quad (4)$$

where  $z$  is the compressibility factor of the gas. Applying eqn. (4) to both Dalton and Amagat's laws gives the compressibility factor of the gas mixture as

$$\text{Dalton:} \quad z_m(P, T) = \sum_i x_i z_i(P_i, T_m) \quad (5)$$

$$\text{Amagat:} \quad z_m(P, T) = \sum_i x_i z_i(P_m, T_m) \quad (6)$$

where  $z_m$  and  $z_i$  are the compressibility factors of the mixture and component gases, respectively, and  $x_i = n_i/n$  is the mole fraction of the component gas with respect to the mixture. Equation (5) implies that the compressibility factor of a gas mixture is approximated by the weighted average of the compressibility factors of the components, each evaluated at the appropriate partial pressure [5]. In contrast, eqn. (6) implies the compressibility factors of the component gases are evaluated at the total pressure of the mixture.

The test gas used in these experiments is a mixture of sulfur hexafluoride ( $\text{SF}_6$ ) and helium (He). The concentration of each gas in the mixture, if evaluated using eqn. (5), is approximately 50%  $\text{SF}_6$  and 50% He. On the other hand, if the properties are evaluated using eqn. (6), the concentration of  $\text{SF}_6$  and He is approximately 55% and 45%, respectively.

### 2.1 Shock Wave Theory

Creation of shock waves in a shock tube can be considered as a one-dimensional Riemann problem [6]. Initially, two gases at different pressures are separated by a thin membrane (or diaphragm). At time  $t = 0$ , the membrane is removed and the gases are allowed to come into contact. At this instant, a disturbance is formed as the high-pressure gas moves towards the low-pressure gas. This original disturbance splits into two opposite waves: a rarefaction (or

expansion) wave and a compression (or shock) wave. The rarefaction wave, which expands the gas at higher pressure, grows thicker while the shock wave, traveling through the low-pressure gas at supersonic speed, grows thinner [7], accelerating and compressing the fluid. Shock waves can be described as discontinuities in fluid flow, in which properties such as density, pressure, and temperature increase instantaneously across the shock front. Since the regime is supersonic, properties in the low-pressure gas (downstream of the shock wave) remain constant until the shock passes.

Generally, in shock wave analysis, a control volume is established containing the shock region and an infinitesimal amount of fluid on each side of the shock [8]. Applying the conservation equations for mass, momentum, and energy to this control volume (assuming steady, one-dimensional, adiabatic flow) will result in three governing equations:

$$\rho_1 u_1 = \rho_2 u_2 \quad (7)$$

$$p_1 + \rho_1 u_1^2 = p_2 + \rho_2 u_2^2 \quad (8)$$

$$h_1 + \frac{1}{2} u_1^2 = h_2 + \frac{1}{2} u_2^2 \quad (9)$$

where  $\rho$  is the density of the fluid,  $u$  is the fluid velocity,  $p$  is the pressure and  $h$  is the enthalpy. The subscripts 1 and 2 correspond to conditions before (downstream) and after (upstream) the shock, respectively. Equations (7) through (9) are referred to as the shock wave equations. The unknown variables in this case are  $\rho_2$ ,  $p_2$ ,  $u_2$ , and the difference in enthalpy  $\Delta h = h_2 - h_1$ . Therefore, an additional equation is needed to solve the problem; the change in enthalpy equation, which is given by

$$dh = c_p dT + (1 - \alpha T) v dp \Rightarrow \Delta h = \int_1^2 c_p dT + \int_1^2 (1 - \alpha T) v dp \quad (10)$$

where  $c_p$  represents the specific heat at constant pressure,  $\alpha$  is the isobaric thermal expansion coefficient,  $T$  is the temperature, and  $v$  is the specific volume [6]. In order to characterize the properties of the gas mixture, eqn. (10) requires the application of a thermodynamic model, such as either Dalton's law or Amagat's law. However, if the temperature  $T_2$ , pressure  $p_2$ , and velocity  $u_2$  can be determined experimentally, eqns. (7)–(10) can be solved directly and compared to theoretical predictions from both thermodynamic models.

Pressure measurements in a shock tube are relatively simple to acquire, through the use of high-frequency response pressure transducers (PTs). Various models and configurations of these transducers are commercially available. Temperature on the other hand, is a completely different story. The use of a thermocouple probe is an invasive procedure, which could drastically alter flow physics. Furthermore, there exist no commercially available thermocouples that possess the necessary response time (on the order of microseconds) and are robust enough to survive conditions within the shock tube. An alternative method of temperature measurement is required. This method must be non-invasive, so as to not disturb the flow within the shock tube, and it must have ultra-fast response times to accurately measure temperature across the shock wave. Infrared (IR) detectors offer a solution to both of these problems. They provide line-of-sight measurements of average temperature within the shock tube, and characteristic response times on the order of nanoseconds.

What follows is a description of an experimental setup in the Shock Tube Facility at the University of New Mexico Mechanical Engineering Department in which an infrared

detector is used to provide temperature measurements both before and after shock passage. These experimental results are then compared with theoretical predictions of Dalton's law and Amagat's law in an effort to determine which law is more suitable for gas mixtures.

### 3 EXPERIMENTAL ARRANGEMENT AND DIAGNOSTICS

The infrared detector used in these experiments (manufactured by InfraRed Associates, Inc.) utilizes an ultra-fast response liquid nitrogen (LN<sub>2</sub>) cooled photo-conductive mercury cadmium telluride (MCT) sensor, with a nominal operating temperature of 77 K. A response time of 60 nanoseconds makes this type of thermal sensor ideal for experiments conducted in a shock tube. However, each sensor is unique to the gas mixture tested and information about the infrared absorption (or transmission) spectrum of the gas itself is necessary. In order to obtain accurate results (and due to the sensitivity of the sensor itself), only a small fraction of the IR spectrum should be considered. This is accomplished by the use of a Germanium narrow band-pass filter mounted on the front of the sensor housing. Preliminary research [9] shows that peak absorption (~98%) of IR in sulfur hexafluoride (SF<sub>6</sub>) occurs between  $\lambda = 10 \mu\text{m}$  and  $\lambda = 11 \mu\text{m}$  wavelength. However, absorption drops to ~80% in the range  $7.5 \mu\text{m} \leq \lambda \leq 8.5 \mu\text{m}$ . This wavelength range was chosen in an effort to properly characterize the amount of IR light transmitted (and absorbed) through the test gas.

LN<sub>2</sub>-cooled IR sensors of this type measure line-of-sight transmission of infrared radiation. As the transmission of light through a participating medium decreases, the corresponding signal from the detector also decreases (which implies absorption of IR radiation increases). In order to analyze signals from the detector, it must be calibrated using the test gas, with known temperatures and pressures. Consequently, a calibration experiment was devised and implemented prior to any experiments conducted on the shock tube. Figure 1 shows the

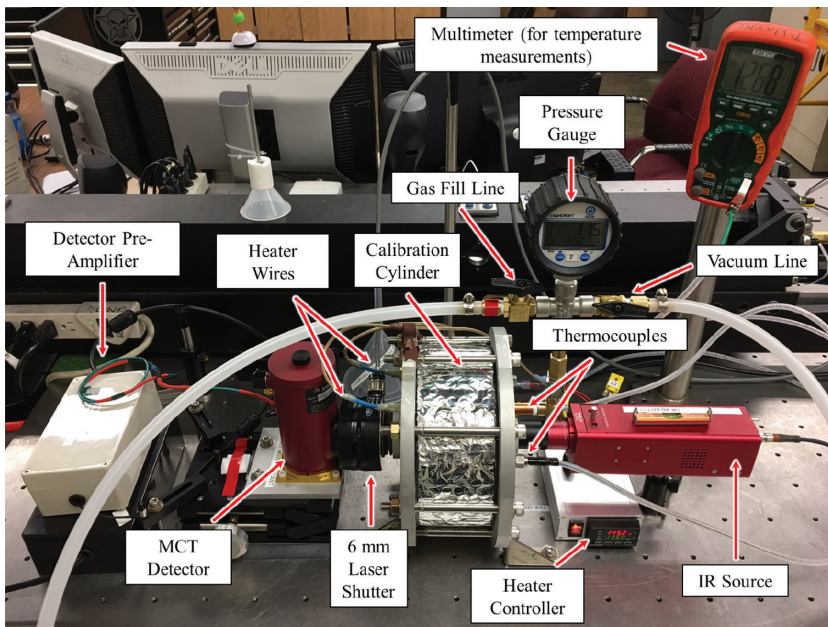


Figure 1: Experimental setup used to calibrate the MCT detector.

calibration experiment. The calibration cylinder seen in the center of the image consists of six main components: a small aluminum cylinder (4" in diameter, 0.5" thick) wrapped in an ultra-high temperature heater tape, a larger aluminum cylinder (7" in diameter, 0.5" thick), two aluminum side plates, and two optical window mounts housing zinc selenide (ZnSe) windows, which operate as bandpass filters for infrared wave-lengths between  $\lambda = 7 \mu\text{m}$  and  $\lambda = 12 \mu\text{m}$ . The linear distance between the inner faces of the ZnSe windows is exactly 3 inches, which corresponds to the distance between the inside walls of the shock tube. The radiation source used in both the calibration and shock tube experiments is a Thorlabs SLS203L compact stabilized broadband infrared light source, with a color temperature of 1500 K.

### 3.1 Calibration Procedure

Prior to each calibration experiment, the IR source is activated and allowed to stabilize for approximately 45 minutes. The glass dewar housing the MCT detector (Fig. 1) is filled with liquid nitrogen and stabilized during this time period. If high temperature readings are needed, the heater tape is also activated via a PID (proportional-integral-derivative) heater temperature controller and allowed to reach thermal equilibrium at the prescribed temperature. The MCT detector and IR source are aligned perpendicular to the optical windows along the same axis. A Vincent Associates Uniblitz LS6 laser shutter (6 mm aperture, 1.7 ms open time) is placed along the optical axis in front of the MCT detector, which effectively simulates an instantaneous increase in temperature, as would be seen by the sensor when the shock wave passes. To maintain repeatability and reduce sources of error, the detector, shutter, and IR source are anchored in the same configuration for the duration of the calibration experiments.

The procedure begins with a thorough mixing of the SF<sub>6</sub>/He test gas. The calibration cylinder inner chamber is completely evacuated using a vacuum pump (assuming a near-perfect vacuum). The gas mixture is then injected into the cylinder chamber to one of ten prescribed operating pressures. The laser shutter can then be activated at any time, allowing infrared radiation to pass from the source, through the test chamber containing the gas mixture, and onto the MCT sensor, located on the front of the glass dewar. The pre-amplified electrical signal from the detector is sent to a National Instruments USB-5132 digital oscilloscope and read by corresponding NI-Scope software. The signal (measured in Volts) from the detector is proportional to the amount of infrared radiation transmitted through the test gas (via emission from the gas itself and from the IR source). Assuming the test gas follows the theory of infrared absorption spectroscopy, the signal from the detector should decrease as the temperature of the gas in the calibration chamber increases.

Two thermocouples, mounted parallel to the optical axis, are placed inside the calibration cylinder test chamber. One thermocouple measures the temperature of the gas mixture, the other is used by the heater PID controller to maintain the desired set temperature. Eight prescribed calibration temperatures were chosen, starting from room temperature (~22 C) to approximately 160°C, in 20°C increments. Six samples were taken for each pressure/temperature combination. The calibration pressures were chosen according to previous experiments of this type [6]; these pressures range from 39.00 kPa to 593.0 kPa.

### 3.2 Shock Tube Procedure

Figure 2 is an image showing the collective components used for conducting experiments in the shock tube. In order to maintain consistency, the infrared detector, ZnSe optical windows,

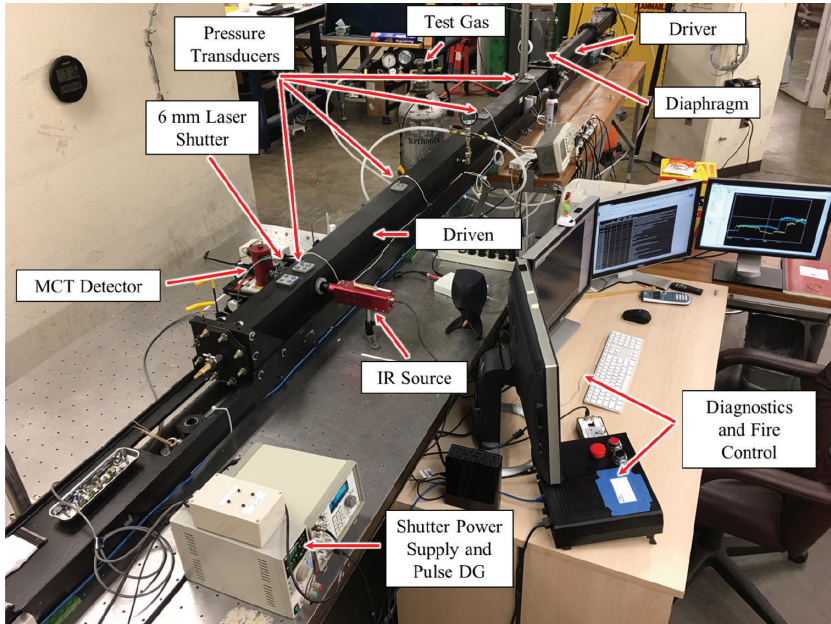


Figure 2: Shock tube experimental setup showing the driver and driven sections of the tube as well as the configuration of the detector and infrared source, located coincident with the 4th downstream pressure transducer.

infrared light source, and laser shutter are arranged in the exact same configuration as was used in the calibration experiment (including matching distances between components).

In the current configuration, the shock tube consists of two main sections, the driver section and the driven section. During each experiment, the driver and driven sections are separated by a thin-film (0.01" thick) polyester diaphragm. Each section is then evacuated using a vacuum pump until an assumed near-perfect vacuum is reached. The driver section is then filled with nitrogen to a predetermined pressure (1010 kPa, 1140 kPa or 1280 kPa) depending on the desired strength (or Mach number) of the shock wave. Once this pressure has been reached, the driven section is pressurized with the SF<sub>6</sub>/He gas mixture to one of three prescribed pressures: 39.00 kPa, 79.00 kPa and 118.0 kPa (monitored by a digital pressure gauge, accurate to 0.25%). For reference, these correspond to the initial conditions for each test. Once this pressure has been reached and the driven section is allowed to stabilize, a pneumatically-driven stainless steel rod, tipped with a broad arrowhead is fired into the diaphragm, sending a planar shock down the length of the driven section. Four high-frequency response pressure transducers located on the top of the driven section record the pressure pulse from the shock wave as it passes. These data can then be used to determine the shock speed ( $u_2$ ) and corresponding pressure jump across the shock front (via manufacturer-supplied calibration curves).

Ambient temperature readings ( $T_1$ ) of the test gas (via the MCT detector) are taken just prior to the shot. These data, when combined with readings of temperature after shock passage ( $T_2$ ), are used to determine the actual temperature jump across the shock front. The location of the detector is coincident with the position of the 4th pressure transducer, downstream of the diaphragm.

#### 4 RESULTS AND DISCUSSION

What follows is a summary of the process used to analyze and plot calibration curves for the detector, according to the prescribed pressure in the calibration cylinder. Calibration curves were obtained for each prescribed chamber pressure, both with and without radiation from the IR source. This allows characterization of IR emission from the test gas as well as absorption of infrared light.

The outline for shock tube experiments consists of testing three separate Mach numbers, each paired with three different initial pressures (39.00 kPa, 79.00 kPa, 118.0 kPa) in the driven section of the shock tube. To clarify, the pressure in the driver section depends on the desired strength (or Mach number) of the shock wave; either 1010 kPa, 1140 kPa or 1280 kPa. However, the actual speed of sound in the mixture is unknown. Therefore, the Mach number in each experiment can only be determined through post-processing and analysis.

Previous experiments [6] have shown that the pressure across the shock front,  $p_2$  varies according to the strength of the shock wave and the initial conditions inside the driven section. In order to obtain accurate measurements of post-shock temperature  $T_2$  during experiments, the infrared detector must be calibrated at each known value of  $p_2$ . Table 1 outlines the various pressures tested during the calibration process.

Each data sample was imported into Matlab and filtered using a 50-point moving average Savitzky-Golay smoothing algorithm to reduce noise in the signal. Figure 3 is an example of the application of this algorithm, showing a drastic reduction in signal noise. The maximum value of each processed signal was determined and used to plot calibration curves. In order to minimize error, only the first 2 ms of the 10 ms total time window were chosen. These curves will be used to analyze temperature (and pressure) data obtained in the shock tube experiments.

Figure 4 is a calibration curve (both with and without the IR source) corresponding to a calibration cylinder chamber pressure of 331.0 kPa. The  $x$ -axis is the temperature within the chamber ( $^{\circ}\text{C}$ ), and the  $y$ -axis is the signal from the detector (V). Upward-facing triangles correspond to data obtained with the IR source, while dark blue squares correspond to data

Table 1: Pressures tested in the calibration process, according to driver pressure and initial conditions.

$p_{driver}$ (kPa)	Initial Conditions ( $p_1$ )	Calibration Chamber Pressure ( $p_c$ )
1010	39.00 kPa	331.0 kPa
1010	79.00 kPa	386.0 kPa
1010	118.0 kPa	421.0 kPa
$p_{driver}$ (kPa)	Initial Conditions ( $p_1$ )	Calibration Chamber Pressure ( $p_c$ )
1140	39.00 kPa	386.0 kPa
1140	79.00 kPa	469.0 kPa
1140	118.0 kPa	510.0 kPa
$p_{driver}$ (kPa)	Initial Conditions ( $p_1$ )	Calibration Chamber Pressure ( $p_c$ )
1280	39.00 kPa	421.0 kPa
1280	79.00 kPa	545.0 kPa
1280	118.0 kPa	593.0 kPa

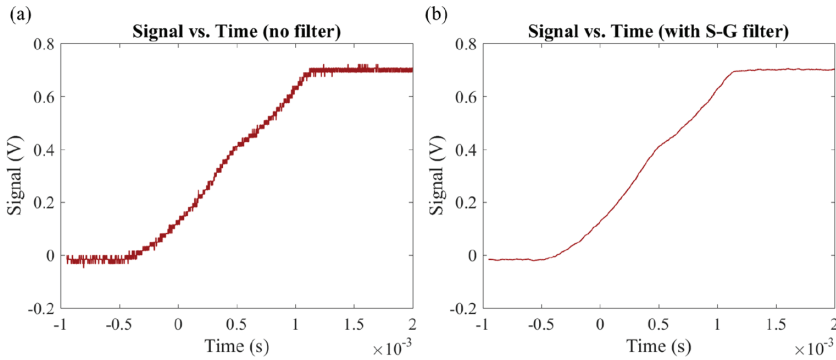


Figure 3: A sample signal from the MCT detector shown (a) before and (b) after application of the Savitzky-Golay smoothing algorithm.

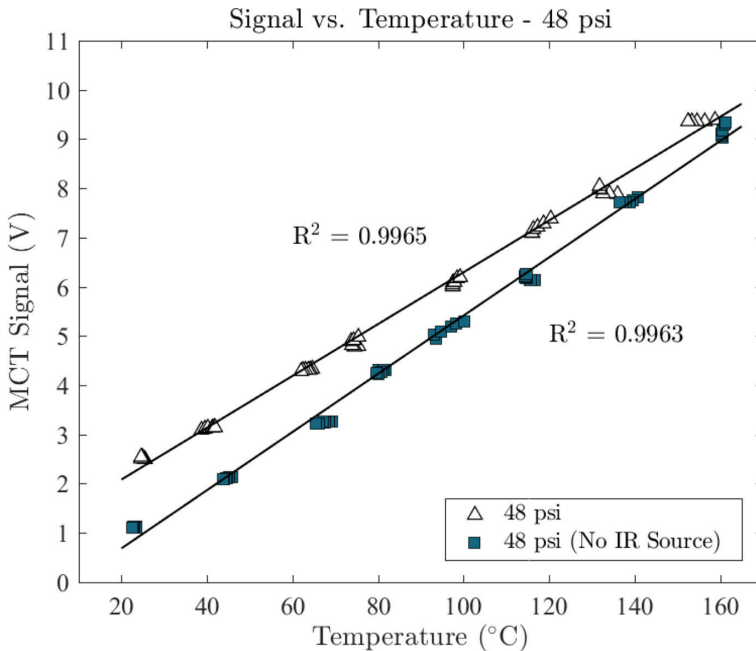


Figure 4: Calibration curve(s) generated using Matlab for 331.0 kPa calibration cylinder chamber pressure. Upward facing triangles correspond to measurements taken with the infrared source and dark blue squares correspond to measurements taken with the source. Six samples at each temperature increment were taken.

obtained without the IR source (self-emission of infrared from the test gas itself). Correlation coefficients ( $R^2$ ) for both curves are also shown to demonstrate highly accurate linear curve fits.

## 5 FUTURE WORK

As this research is ongoing, future work will include experimental measurements of post-shock temperature in a gas mixture of sulfur hexafluoride and helium, subject to a moving

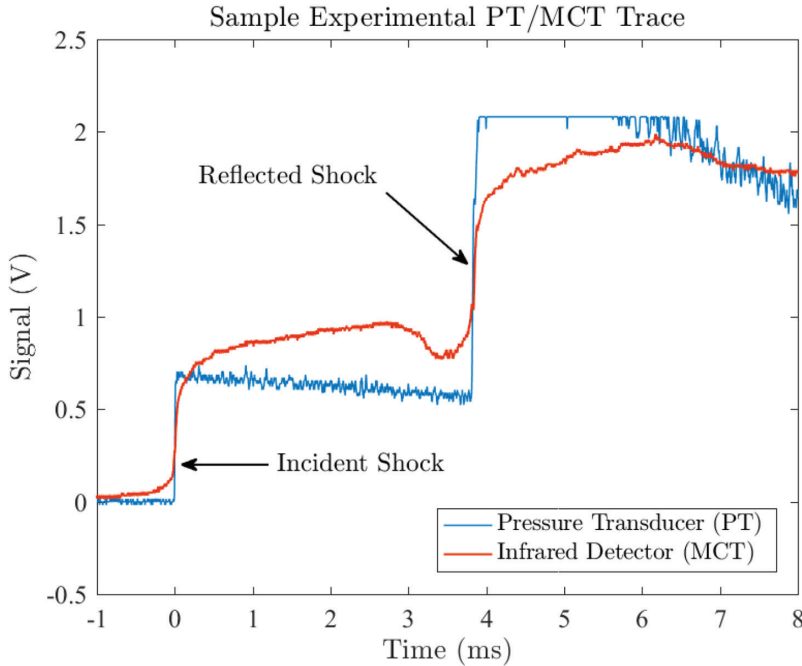


Figure 5: Sample graph of the pressure and temperature traces obtained in a shock tube experiment, with a driver pressure of 1140 kPa. The pressure of the test gas in the driven section was 79.00 kPa (local atmospheric pressure).

normal shock. Figure 5 is a preliminary sample trace showing the response of the 4th downstream pressure transducer (blue line) and MCT detector (red line). Note that the MCT detector is placed coincident with the location of the pressure transducer. Here, increases in signal correspond to higher values of pressure and temperature. Driver and driven (test) pressures for this experiment were 1140 kPa and 79.00 kPa, respectively.

Several concentrations of each component gas will be tested, including mixtures of 25%/75% and 75%/25% SF<sub>6</sub>/Helium by mole, respectively. These data will be used to calculate speed of sound in the mixture and corresponding Mach number of the shock wave. The results will be compared with theoretical predictions using both Dalton's law of partial pressures and Amagat's law of partial volumes, in an effort to determine which law is more suitable.

#### ACKNOWLEDGMENT

This research is supported by the US National Nuclear Security Administration (NNSA) grant DE-NA-0002913.

#### REFERENCES

- [1] Dalton, J., Essay IV. On the expansion of elastic fluids by heat. *Memoirs of the Literary and Philosophical Society of Manchester*, **5**, 1802.
- [2] Çengel, Y.A., Cimbala, J.M. & Turner, R.H., *Fundamentals of Thermal-Fluid Sciences*, chapter 24. McGraw-Hill, New York, New York, 4th edition, 2011.

- [3] Ran H. & Mavis, D., *Preliminary design of a 2d supersonic inlet to maximize total pressure recovery* (volume AIAA 2005-7357). Arlington, Virginia, AIAA 5th Aviation, Technology, Integration, and Operations Conference (ATIO), 2005.
- [4] Liang, Z., Curran, T. & Shepherd, J.E., *Structural response to detonation loading in 90-degree bend*, Springer Berlin Heidelberg, Berlin, Heidelberg, pp. 383–388, 2009.
- [5] Woo, K.W. & Yeo, S.I., Dalton's law vs. Amagat's law for the mixture of real gases. *The SNU Journal of Education Research*, pp. 127–134, 2011.
- [6] Monje, I.T. & Yoo, J.H., *Investigation of Dalton's law and Amagat's law for mixtures using shock wave propagation*. Arlington, Texas, AIAA Region IV Student Conference, 2016.
- [7] Krehl, P.O., *History of Shock Waves, Explosions and Impact: A Chronological and Biographical Reference*, chapter 3. Springer-Verlag, New York, New York, 2008.
- [8] Zucker, R.D. & Biblarz, O., *Fundamentals of Gas Dynamics*, John Wiley and Sons, Inc., Hoboken, NJ, 2002.
- [9] Lagemann, R.T. & Jones, E.A., The infrared spectrum of sulfur hexafluoride. *The Journal of Chemical Physics*, **19**(5), pp. 534–536, 1951.  
<https://doi.org/10.1063/1.1748287>